Small fish biomass limits the catch potential in the High Seas

J. Guiet[1], D. Bianchi[1], K.J.N. Scherrer[2], R.F. Heneghan[3,4]and E.D. Galbraith[5]

[1]Department of Atmospheric and Oceanic Sciences, University of California Los Angeles, CA, United States
[2]Department of Biological Sciences, University of Bergen, 5020 Bergen, Norway
[3]Australian Rivers Institute, School of Environment and Science, Griffith University, Nathan, Australia
[4]School of Science, Technology and Engineering, University of the Sunshine Coast, Petrie, Australia
[5]Earth and Planetary Science, McGill University, Montreal, QC, Canada

Key Points:

- Despite their vast surface area, the High Seas provide only a small fraction of global wild fish catch.
- Dispersion of trophic energy throughout deep water columns and micronutrient limitations leads to smaller fish biomass density in High Seas.
- Smaller biomass density is a major contributor to the small catch; while migration should also matter, economic factors are likely secondary.

Corresponding author: Jerome Guiet, `jerome.c.guiet@gmail.com`

Abstract

The High Seas, lying beyond the boundaries of nations' Exclusive Economic Zones, cover the majority of the ocean surface and host roughly two thirds of marine primary production. Yet, only a small fraction of global wild fish catch comes from the High Seas, despite intensifying industrial fishing efforts. The surprisingly small fish catch could reflect economic features of the High Seas - such as the difficulty and cost of fishing in remote parts of the ocean surface - or ecological features resulting in a small biomass of fish relative to primary production. We use the coupled biological-economic model BOATS to estimate contributing factors, comparing observed catches with simulations where: (i) fishing cost depends on distance from shore and seafloor depth; (ii) catchability depends on seafloor depth or vertical habitat extent; (iii) regions with micronutrient limitation have reduced biomass production; (iv) the trophic transfer of energy from primary production to demersal food webs depends on depth; and (v) High Seas biomass migrates to coastal regions. Our results suggest that the most important features are ecological: demersal fish communities receive a large proportion of primary production in shallow waters, but very little in deep waters due to respiration by small organisms throughout the water column. Other factors play a secondary role, with migrations having a potentially large but uncertain role, and economic factors having the smallest effects. Our results stress the importance of properly representing the High Seas biomass in future fisheries projections, and clarify their limited role in global food provision.

1 Introduction

The UN High Seas Treaty, agreed upon in March 2023, has been welcomed as an unprecedented step towards protecting the biodiversity of the global ocean (UN General Assembly, 2023). Known as the Biodiversity Beyond National Jurisdiction treaty, it explicitly calls for an integrated ecosystem approach in order to maintain and restore biodiversity and carbon cycle functioning within the 60% of the ocean area that lies beyond nationally-managed Exclusive Economic Zones (EEZs). A fundamental metric of the biodiversity that the treaty aims to protect is the abundance or biomass of marine organisms. However, because of the inaccessibility of the High Seas, and the fact that they falls outside the purview of national research organizations, the biomass of animals in the High Seas is relatively poorly evaluated.

The oceans are thought to harbour most of the remaining wild animal life on the planet (Bar-On et al., 2018). Since the High Seas cover the majority of the ocean surface, one could expect them to host a large fraction of marine life. Consistent with this expectation, roughly 67% of marine primary production is estimated to occur in the vast domain of the High Seas, even though the rate of primary production per unit area is higher in the shallow coastal waters that ring the continents (Behrenfeld & Falkowski, 1997; Carr et al., 2006; Marra et al., 2007). Given that roughly half of global primary production is marine, this implies that one third of all primary production on Earth occurs in the High Seas. Yet, the most comprehensive sampling of marine animals by humans - industrial fishing - recovers only a small fish catch from the High Seas, despite intensifying efforts (Rousseau et al., 2019). In fact, humans only retrieve about a twen-

tieth of the global wild fish capture – less than 0.1% of total human caloric supply – from the High Seas that cover more than half the planet (Schiller et al., 2018). We are not aware of a widely-recognized explanation for the fact that the High Seas provide so little human food.

On one hand, the surprisingly small High Seas catch could be explained by economic and technological constraints. Fuel and time expenditures required to travel long distances, greater capital requirements for High Seas vessels, or the difficulty of catching fish in deep waters could result in higher costs of fishing the High Seas (Lam et al., 2011; Sala et al., 2018). Economic constraints can be further modulated by the variable catchability of the fish resource that is influenced by habitat features such as topography, or vary between gears targeting pelagic or demersal species (Palomares & Pauly, 2019; Kerry et al., 2022). On the other hand, the small fish catch relative to primary production could be a result of ecological features of the High Seas. It is possible that the High Seas have less efficient transfer of energy from primary production to fish types of commercial interest compared to coastal systems (Eddy et al., 2020), or that primary production in the High Seas is consumed by fish that periodically migrate to the coastal zone, leading to spatial redistribution of the biomass of upper trophic levels (Block et al., 2011; Sumaila et al., 2015). To our knowledge, these alternatives have not been investigated in a consistent, integrated framework.

In recent years, a new generation of numerical marine ecosystem models offers a novel means to address the chronic undersampling of the High Seas. These models do not attempt to resolve individual species, but instead use fundamental empirical ecological processes to predict the growth and life history of generalized fish communities from features of the environment, including water temperature and resources from lower trophic levels, such as primary production and zooplankton biomass (Maury, 2010; Guiet et al., 2016; Blanchard et al., 2017; Tittensor et al., 2018; Heneghan et al., 2021). While these models have been designed and parameterized based on the rich observational datasets available for coastal fisheries (RAM Legacy Stock Assessment Database, 2020; Watson, 2017; Pauly et al., 2020), it is possible to use their ecological principles to make predictions for fish production and biomass in the High Seas.

Figure 1 shows predictions from the Fisheries and Ecosystem Model Intercomparison Project (FishMIP) ensemble (Tittensor et al., 2018, 2021) for the High Seas (HS) compared to coastal seas (CS). All of them estimate a fraction of High Seas biomass, B, relative to the global ocean surface area and primary production in the High Seas: around 60% in the 1990s, the decade when global fish catches peaked (FishMIP bar in Fig. 1a, see also Appendix A to compare models). Among these models, the BOATS model simulates fish catches, C, in addition to biomass by including a coupled economic module that allocates fishing effort dynamically based on the profitability of fishing at a given time in the global ocean (Carozza et al., 2016, 2017). BOATS predicts that the HS fraction of catch is less than that of biomass, but nonetheless far above observations at 35% of global catches in the 1990s (in blue in Fig. 1a). Furthermore, the model incorrectly simulates substantial growth in the High Seas catch and biomass fractions since 1950 (deep and light blue lines in Fig. 1b). However, both the initial High Seas catch ratio and its

rate of increase in BOATS greatly exceeds observations (black lines in Fig. 1a,b; catch reconstruction by Pauly et al., 2020, dashed line, and Watson, 2017, dotted line).

Here, we use the BOATS model and implemented new processes to test five hypotheses that could contribute to the discrepancies between observed and modeled High Seas catches, indirectly shedding light on the global commercial biomass distribution (see Table 1). The first two hypothesis are economic, testing the degree to which lower profitability of High Seas fishing can reasonably explain the low catches (Lam et al., 2011; Palomares & Pauly, 2019). The inherently higher cost involved with travelling to the deep sea, and operating gear in deep waters is explored through the hypothesis HIGHCOST. It is also conceivable that a greater dispersal of fish in the vast and deep high-seas makes it more difficult to catch the existing biomass, tested in hypothesis UNCATCHABLE. Three additional hypotheses focus on ecological reasons why there may be less biomass available in the High Seas than would be expected from primary production and water temperature alone. The limitation of phytoplankton growth because of iron limitation in high-nutrient low-chlorophyll (HNLC) regions is widely recognized (Moore et al., 2013; Tagliabue et al., 2017). While micronutrient limitation of higher trophic levels, including fish, remains unclear, multiple lines of evidence suggest that iron limitation could also retard or prevent growth of fish in the High Seas (Galbraith et al., 2019). This is captured in the IRONLIM hypothesis. The ENERGYPATHS hypothesis distinguishes between pelagic and benthic energy pathways, to test the possibility that deep waters produce little fish biomass because the energy of primary production is dissipated in the water column before reaching benthic communities, and preferentially routed to small organisms (Stock et al., 2017; van Denderen et al., 2018). Finally, the MIGRATION hypothesis explores the possibility that seasonal migrations deplete the High Seas of biomass by bringing "straddling" stocks into coastal waters, where they are more accessible to fishers. Straddling species represent a significant fraction of total catches (White & Costello, 2014; Sumaila et al., 2015), but the fraction of biomass of these catches produced in the High Seas is unknown.

Table 1. List of hypotheses tested to explain the observed low High Seas vs. coastal catches and their expected effect on key variables, cost, catchability and biomass (see details Material and Methods).

Hypothesis	Cost (c)	Catchability (q)	Biomass (f)
HIGHCOST (S_{cost})	↑ with distance/depth	-	-
UNCATCHABLE (S_{catch})	-	↓ with depth	-
IRONLIM (S_{iron})	-	-	↓ in HNLC regions
MIGRATION (S_{mig})	-	-	↓ in HS, ↑ in CS
ENERGYPATHS (S_{ener})	-	-	↓ with depth

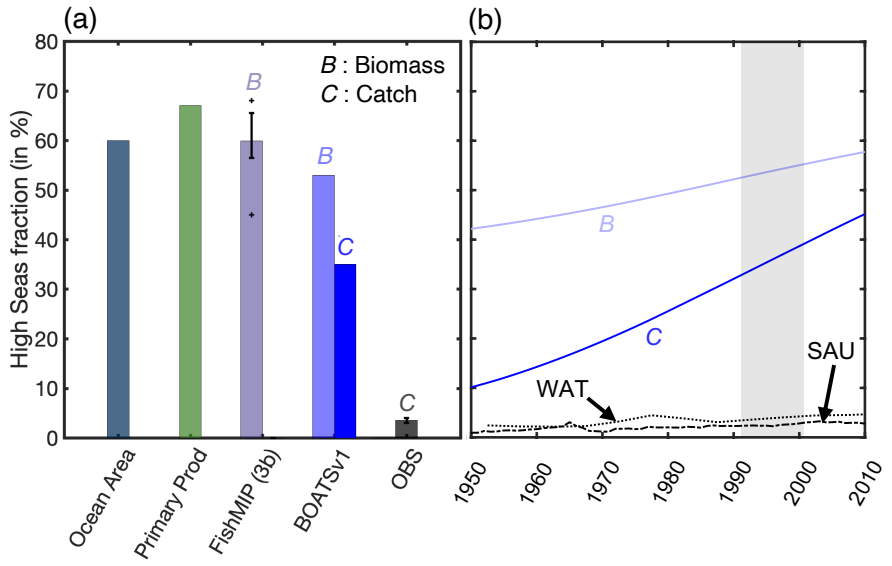

Figure 1. Contribution of the High Seas to the global total. (a) The High Seas fraction (%) of global ocean surface area, primary production, simulated biomass B and catch C, in the 1990s for 8 models of the FishMIP ensemble (APECOSM, DBPM, EcoOcean, EcoTroph, FEISTY, Macroecological, ZooMSS), BOATSv1, and observed catch (OBS). (b) Historical evolution of biomass, B, and catch, C, for BOATSv1 and observations. Observations are based on catch reconstructions from the Sea Around Us (SAU, dashed, Pauly et al., 2020) and Watson (2017) (WAT, dotted). The gray shading panel (b) indicates the time period used for comparisons in panel (a) and Figure 2.

2 Material and Methods

2.1 Mechanistic modeling framework

To test our hypotheses (Table 1), we use the coupled ecological-economic global marine ecosystem model BOATS to predict fish biomass and catches in the High Seas and coastal waters from environmental and economic drivers (Carozza et al., 2016, 2017). We conducted this analysis using the original BOATSv1 model and an updated version that incorporates several new features, referred to as BOATSv2 (Guiet et al., 2024).

BOATS simulates the dynamics of commercial fish biomass, dependent on available resources at the base of the food web. Mean water temperature modulates the rate of biomass propagation across food webs, including production and losses. BOATS is dynamically coupled with an open-access economic module that allow simulations of fishing effort and catch dynamics. Previous work with BOATSv1 showed that the model, forced with globally homogeneous fishing costs and catchability, is able to reproduce the historical development of fisheries when driven by a uniform technological creep (3 to 8% per year, Galbraith, Carozza, & Bianchi, 2017; Guiet, Galbraith, Bianchi, & Cheung, 2020). In the following sections, we discuss a series of modifications of BOATSv1 and new simulations aimed at examining our five key hypotheses.

2.1.1 HIGHCOST

In BOATSv1, the cost per unit effort (c, in $\$/W/yr$) is globally uniform by default. The absence of spatial dependence of cost disregards the importance of transit distance between fishing grounds and ports (Sala et al., 2018), which might be particularly relevant when comparing High Seas and coastal catches. In addition, costs are expected to rise when targeting increasingly deep fishing grounds, due to depth-dependent expenses associated with setting and hauling gears. Since demersal catches account for a large fraction of global catches, this might contribute to the delayed development of High Seas catches as deeper offshore habitats might become profitable later in time (Watson & Morato, 2013). We test both types of variable cost distributions independently under the HIGHCOST hypothesis.

For implementation, we assume that the fishing cost per unit effort is constant in coastal or shallow regions ($c = c_{CS}$). Beyond these regions, the cost increases linearly, either as a function of distance to the nearest shore (d_{coast}, in km), or as a function of seafloor depth (z_{bot}, in m):

$$c(x = d_{coast}, z_{bot}) = \begin{cases} c_{CS} \quad \text{when} \quad x \leq x^* \\ c_{CS} + \delta_c(x - x^*) \quad \text{when} \quad x > x^* \end{cases} \tag{1}$$

where x represents either d_{coast} or z_{bot}, x^* is a reference value that indirectly determines the boundary of coastal regions, and δ_c is a parameter controlling the rate of increase of costs beyond coastal regions (in $\$/km/W/yr$ or $\$/m/W/yr$, for distance to coast or bottom, respectively). We note that calculating distance to the nearest shore to mod-

ulate costs is a simplification, particularly for industrial fisheries. We test multiple sets of parameters [x^*, δ_c] (see Appendix B).

2.1.2 UNCATCHABLE

Catchability (q, in $m^2/W/yr$) refers to the capturability of fish biomass per unit effort given fish behavior (e.g. schooling, gear avoidance) and the level of technology, including fishing gear, navigation technologies, sonar, communications and skipper knowledge. Catchability generally grows exponentially over time through technological progress (Palomares & Pauly, 2019; Eigaard et al., 2014), thus driving the historical development of fisheries (Galbraith et al., 2017). However, the globally uniform catchability increase in BOATSv1 does not account for geographical variations in the marine environment, which could be significant. For example, pelagic fish in regions with vertically compressed euphotic zones might be more accessible to purse seines than in regions where production is spread over a larger, more diffuse vertical range (Nuno et al., 2022). Under the UNCATCHABLE hypothesis, we incorporate spatially varying catchability to assess how this might affect catches.

First, we test the scenario in which catchability varies as a function of the euphotic layer depth (z_{eu}, in m). Second, we test the scenario in which catchability varies as a function of seafloor depth (z_{bot}, in m), based on the notion that shallower regions, such as those around seamounts or on continental shelves, promote biomass aggregation (Kvile et al., 2014) and enhance fisheries' access to marine fish stocks (Kerry et al., 2022). The UNCATCHABLE hypothesis tests both variable catchability distributions:

$$q(x = z_{eu}, 1/z_{eu}, z_{bot}, 1/z_{bot}, log_{10}(z_{bot})) = q_{ref}\left[q_{min} + (1 - q_{min})\frac{x_{max} - x}{x_{max} - \overline{x}}\right] \quad (2)$$

Here x represents a function of either euphotic zone or seafloor depth, x_{max} the global maximum of the quantity, $\overline{x}$ the global mean, and q_{min} is a parameter that controls the change of catchability as a function of depth. Note that we test formulations in which catchability decreases either linearly or in proportion to the inverse of either the euphotic zone depth or the seafloor depth (see Appendix C). In each formulation, we select q_{min} values that provide realistic spatial variations, and use $5\times q_{min}$ as an upper bound to catchability, effectively limiting its variation to the observed range (Palomares & Pauly, 2019). The formulation in Equation 2 modulates the global reference catchability (q_{ref}), which increases annually at 5% rate.

2.1.3 IRONLIM

To assess the influence of iron limitation on fish growth, we modulate the trophic efficiency α, a key parameter of BOATS that represents the fraction of organic matter incorporated into new tissue at each trophic step:

$$\alpha = \alpha_0 \frac{k_{NO_3^-}}{k_{NO_3^-} + NO_3^-} \quad (3)$$

where surface nitrate concentrations (NO_3^-, in μM) are taken as a proxy for low iron conditions (Moore et al., 2013). Assuming a constant $k_{NO_3^-} = 5\,\mu M$, this formulation smoothly decreases the trophic efficiency relative to the reference value α_0 as nitrate increases (Galbraith et al., 2019).

2.1.4 ENERGYPATH

BOATSv1 calculates fish biomass from vertically integrated net primary production (NPP) and upper water column temperature (T_{75}). These quantities determine fish growth rates, and ultimately biomass accumulation, in a region. While these forcings are relevant for pelagic species, they do not account for the flux of organic material that reaches the seafloor as sinking particles, and sets the production of deep-sea ecosystems and fisheries (Blanchard et al., 2011; Stock et al., 2017; Petrik et al., 2019). Moreover, cooler temperatures at the ocean bottom ($T_{bot} < T_{75}$) result in slower metabolism and production rates for deep-sea species. Both factors – organic material flux and bottom temperature – must influence new fish biomass production in shallow vs. deep waters. To test the effect of distinct drivers of production in pelagic and demersal communities, under the ENERGYPATH hypothesis we expand BOATSv1 to provide a separate representation of pelagic species, forced by NPP and T_{75}, and demersal species, forced by the particle flux at the bottom (PFB) and T_{bot}.

We derive the PFB from surface NPP (Guiet et al., 2024), assuming a typical power-law attenuation of the particle flux below the euphotic zone (z_{euph}):

$$PFB = NPP \cdot pe_{ratio} \cdot (\frac{z_{bot}}{z_{euph}})^{b_a} \tag{4}$$

where $b_a = -0.8$ is the coefficient of attenuation of particle fluxes with depth (Martin et al., 1987) and $z_{euph} = 75$m the average euphotic zone depth, which, for simplicity, we keep constant. The term $(z_{bot}/z_{euph})_a^b$ is computed first at a high resolution, using z_{bot} values from the global topographic dataset ETOPO $1/10^o$ (Amante & Eakins, 2009), and then averaged across each 1^o grid cells of the model. Note that when z_{bot} is shallower than $z_{euph} = 75$m, the seafloor depth is set to be equal to the euphotic zone depth. The particle export at the base of the euphotic zone is determined by an empirical estimate of the particle export ratio (pe_{ratio}), as a function of local surface temperature T_{75} and NPP, following prior work (Dunne et al., 2005).

2.1.5 MIGRATION

At the coarse resolution of the BOATS model (1^o), the horizontal transport of biomass by currents and active movement can be assumed to play a secondary role relative to local biomass production for many fish. However, global catches include a significant fraction of straddling species that can travel large distances (Sumaila et al., 2015). While straddling stocks are caught almost exclusively in coastal waters, some fraction of this biomass is produced from trophic energy foraged in the High Seas. Fish migration and subsequent capture in coastal seas therefore represents a flux of trophic energy from the high seas to coastal waters that is not resolved by BOATS. This biomass flux could con-

tribute to the discrepancy between modelled and observed catches in the High Seas vs. coastal regions.

Unfortunately, the considerable uncertainty in behavioural drivers of fish migration prevents an explicit representation of this biomass redistribution at this time. Thus, unlike the mechanisms described above, we do not include migration as a mechanistic component of the model. Instead, we gauge the effect of fish migrations by estimating a plausible contribution of High Sea biomass to the total catch in each EEZ i, based on the simulated catch (C_i) inside the EEZ, and the fraction of total catch in the EEZ that can be attributed to straddling species ($\alpha_{str,i}$), which we estimate based on observational catch reconstructions (see Appendix D):

$$C_i = C_i^{adj} - \delta_s \alpha_{str,i} C_i^{adj} \tag{5}$$

where C_i^{adj} is the total catch adjusted for straddling species in a given EEZ, and the arbitrary factor δ_s represents the proportion of the catch of straddling species coming from the High Seas. This factor provides an indirect measure of the coastal catch contribution by fish biomass produced in the High Seas. Rearranging terms in Equation 5 provides an estimate of the total catch C_i^{adj} from simulated catch within each EEZ C_i:

$$C_{CS}^{adj} = \sum_{EEZs} C_i^{adj} \tag{6}$$

$$C_{HS}^{adj} = C_{HS} - \sum_{EEZs} (C_i^{adj} - C_i). \tag{7}$$

Ultimately, we use C_{CS}^{adj} and C_{HS}^{adj} as updated coastal and High Seas catches after biomass redistribution by migration of straddling species, as long as $C_{HS}^{adj} > 0$. Given that δ_s is undetermined, we use a range of values to estimate the magnitude of biomass transfer, and add the resulting High Seas-derived straddling catch to the Coastal Catch.

2.2 Simulations

Our five hypotheses (Table 1) are tested with new simulations compared to the reference simulation made with BOATSv1 (shown in blue in Fig. 1, hereafter simulation S_{v1}). In order to capture uncertainty in model parameters, we run each experiment with a small ensemble of 5 different parameter sets (Carozza et al., 2017). We take the ensemble mean as the final result, and when relevant use the spread across the 5 members as a measure of uncertainty.

We first compare means and uncertainties for new simulations that update the reference model to include economic constraints (S_{cost} and S_{catch}, Table 1). Second, we compare new simulations that test the influence of ecological features (S_{iron} and S_{ener}). Because simulation S_{ener} changes the structure of the ecological model, we generated 5 new parameter sets by running a new optimization with a Monte-Carlo ensemble using the BOATSv2 code (Guiet et al., 2024). Similar to the BOATSv1 parameter ensemble, the BOATSv2 parameter sets were selected to best capture global observations including the catch peak aggregated by Large Marine Ecosystems (LMEs), and the spatial variabil-

ity of historical catch maxima in each LME. BOATSv1 and v2 are both tuned based on similar coastal observations, resulting in comparable dynamics in coastal seas. However, they markedly differ in their representation of the High Seas. Finally, we evaluate the role of straddling species by adjusting catch *a posteriori* from the reference simulation (S_{mig}).

Simulations are run on a 1^o global grid, forced with climatological observations of the surface mean temperature between 0 and 75m (T_{75}) and the temperature near the seafloor (T_{bot}) from the World Ocean Atlas (Locarnini et al., 2006). We estimated T_{bot} as the mean temperature in the water column weighted by the fraction of each depth in a model grid cell as reported by ETOPO $1/10^o$ (Amante & Eakins, 2009). For net primary production, we take the average of three satellite-based estimates to capture some of the variability inherent to primary production models (Behrenfeld & Falkowski, 1997; Carr et al., 2006; Marra et al., 2007). To parameterize iron limitation in HNLC regions we take the monthly minimum surface nitrate in the World Ocean Atlas climatology (Locarnini et al., 2006).

2.3 Observational constraints

To evaluate our hypotheses against observations, we use two spatially explicit reconstructions of global catches: SAU, the Sea Around Us from Pauly et al. (2020); WAT, from Watson (2017). Both provide global catches at 1^o resolution from 1950 to 2014, and are corrected for unreported catches. We focus on the following two indicators:

- (i) The fraction of catch occurring in the High Seas relative to the total catch. We compare this ratio around the global catch peak of the 1990s (+/− 5 years around 1996, gray shading in Fig. 1), for which observations suggest a mean value of 3-4% (OBS in Fig. 1a). For each simulation, we average the 11 years of catch around the peak of catch summed across EEZ, and report the mean and spread (10th to 90th percentiles) of the 5 ensemble members.
- (ii) The historical deepening of the global catch. The deepening of catches over time serves as an indicator of the rate at which fisheries develop in deep vs. shallow regions. The mean observed seafloor depth weighted by the local catch in the 1990s is 372m in SAU and 154m in WAT. We compare these estimates with the mean depth for the 11-year period around the catch peak across EEZs in the model simulations, reporting the ensemble mean and spread.

Once the relevant hypotheses are identified, we further evaluate their contribution to global fisheries' development by independently comparing simulated catches with pelagic and demersal catch reconstructions from the SAU (see Appendix E for the definition of demersal and pelagic groups). We also compare regional catch variations across LMEs and 11 High Seas ecosystems when sequentially including new processes (HSEs, Appendix F).

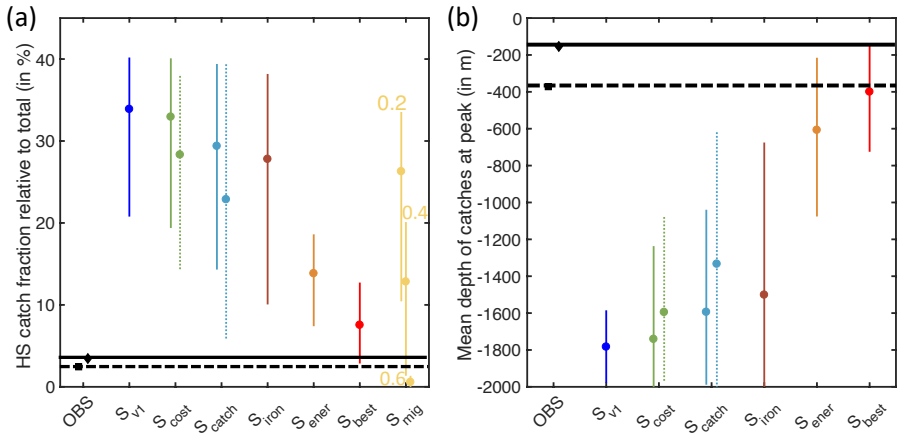

Figure 2. Influence of the hypothesized mechanisms (Table 1) on High Seas fisheries development. (a) Observed and simulated High Seas catch fraction. (b) Observed and simulated mean depth of catches. Values reflect the global catch peak of the 1990s. Simulations are compared with reconstructions from the SAU (black squares and dashed horizontal lines, Pauly et al., 2020) and WAT databases (black diamonds and solid horizontal lines, Watson, 2017). Both panels show the model's ensemble mean and 10-90th percentile range, for each simulation set. In both panels, solid and dotted ranges indicate model variants with distinct parameterizations, i.e., distance- or depth-dependent costs for S_{cost}, euphotic layer- or seafloor- dependent catchability for S_{catch}. In panel (a), for S_{mig}, each range corresponds to a distinct value of the factor δ_s, as reported on the figure.

3 Results and discussion

3.1 Small effect of economic constraints

Both hypotheses related to economic mechanisms (HIGHCOST and UNCATCHABLE) are unable to correct the excessive High Seas catches of the reference simulation S_{v1} when keeping realistic parameterizations (see S_{cost} in green and S_{catch} in light blue, Fig. 2a). Higher fishing costs in the High Seas within the range of observations (i.e., [6.94-8.87]$\$/W/yr$, Sala et al. (2018)) only decrease the fraction of High Seas catches to, on average, 29% (from 35%), while delayed development of fisheries in offshore regions for spatially variable catchability (with deeper euphotic zones and bottom depths) decreases the fraction to 23%. Both remain high compared to the observed 3-4% (see Appendices B,C).

The shift of global catches to shallower fishing grounds is also insufficient for both economic hypotheses (Fig. 2b). But, improvements are substantial, especially when applying depth-dependent fishing costs and catchabilities (Appendices B,C). Access to deep demersal stocks or aggregation of pelagic biomass around seamounts and in shallow regions can contribute to the slow deepening of fishing through time.

3.2 Large effect of energy pathways

Among hypotheses related to ecological mechanisms (IRONLIM and ENERGYPATH), iron limitation of fish partially reduces the mean High Seas catch ratio (down to 28% on average, see S_{iron}, brown line in Fig. 2a). The magnitude is comparable to other economic hypotheses. While allowing the pelagic and demersal communities to develop independently from separate food resources at low trophic levels significantly corrects the fraction (down to 13%, see S_{ener}, orange line in Fig. 2a). These improvements are consistent with a reduced High Seas catch fraction attributable to lower fish biomass production in the High Seas compared to coastal waters.

Similar to other economic constraints, with iron limitation the mean depth of catch remains much deeper than observed (brown line in Fig. 2b). Iron limitation might influence biomass production and thus fisheries yields in the High Seas, yet a link with seafloor depth is lacking. In contrast, having independent pelagic and demersal communities allows a more abundant demersal biomass in shallow waters, which support larger coastal fisheries and ultimately reduces the historical deepening of global catches (orange line in Fig. 2b). Our simulations of the ENERGYPATH hypothesis indicate that it is a fundamental mechanism leading to relatively low catches in the High Seas.

3.3 Combined economic and ecological effects

Taken in isolation, ecological features limiting biomass production in High Seas best explain the smaller High Sea catches (IRONLIM and ENERGYPATH), while economic constraints are insufficient (HIGHCOST and UNCATCHABLE). However, the inclusion of economic constraints could still influence spatio-temporal dynamics.

Historically, observed demersal catches are largely coastal (60 times larger inside EEZ than High Seas in 2000s, compare black solid and dotted lines in Fig. 3a), while pelagic catches are more evenly distributed between coastal waters and the High Seas (20 to 1 in 2000s, Fig. 3b). When the ecological features are implemented in BOATS, they largely capture the historical variation of catch for each functional type, with slight overestimation of High Seas catches (orange lines in Fig. 3). Yet, development of High Seas fisheries still occurs in the model and becomes increasingly over-estimated after 1990. The selected economic constraints mitigate this bias by reducing catch on the more homogeneously distributed pelagic biomass (red lines in Fig. 3). For instance, with depth-dependent demersal fishing costs and depth-dependent pelagic catchabilities, the fraction of High Seas catch reaches 8% for a mean depth of catch of 400m, close to observation (see S_{best} Fig. 2).

Spatially (Fig. 4), the addition of ecological features corrects the simulated catch densities across LMEs and HSEs (from R=0.73 to 0.83, while RMSE is halved, Figs. 4a,b). The correction is especially important in regions over deeper seafloors (compare color shadings in Figs. 4a,b). In shallower coastal regions, yields remain comparable, as pelagic and demersal communities experience similar environmental forcing (compare circles in Figs. 4a,b). In deeper regions, especially in the High Seas, yields drop markedly, in agreement with a lower biomass production (compare darker markers and triangles). Economic

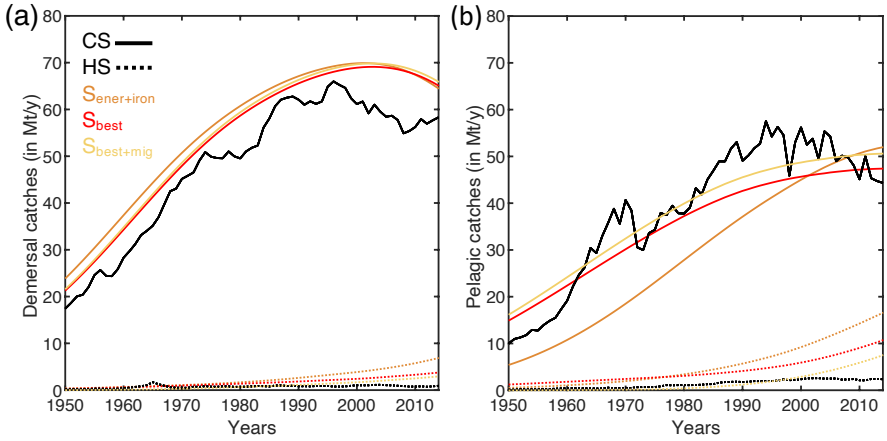

Figure 3. Historical evolution of pelagic and demersal catch. (a) Historical demersal fish catch. (b) Historical pelagic fish catch. In each panel, the solid lines indicate catches inside EEZs, while dotted lines indicate catches in the High Seas. Simulations including ecological corrections ($S_{ener+iron}$ in orange), ecological and economic corrections (S_{best} in red), and correction for straddling biomass ($S_{best+mig}$ in yellow).

features have a smaller effect (correlation from R=0.83 to 0.84, RMSE decreases from 0.16 to 0.11, Figs. 4b,c). The influence of depth on costs and catchability further delays the development of fisheries in High Seas, ultimately reducing yields at the peak in the 1990s (compare triangles in Figs. 4b,c). Economic constraints must have impacted the development of High Seas fisheries, yet their effect on the small High Seas catch fraction is secondary compared to the mechanisms that govern the global fish biomass distribution.

Together, the selected economic and ecological hypotheses explain the variability of global catch with high fidelity (compare spatial distributions in the 1990s, Figs. 4d and e). Notable mismatches remain in the Western Equatorial Pacific, which supports larger fisheries than simulated by the model, and in Arctic waters, where the model overestimates catches. Our definition of economic constraints could influence the mismatches, or these indicate missing processes. New observational metrics will be necessary to weigh the effect of these mechanisms. While fisheries management must also influence regional dynamics (K. Scherrer & Galbraith, 2020), smaller High Seas catches primarily results from lower biomass densities in these regions.

3.4 Migration redistributes biomass

Thus far, we have not addressed the role of migrating fish biomass from High Seas to the coast. Our analysis shows that straddling species, migrating between coastal waters and the High Seas, are caught in many high latitude and subtropical insular EEZs, where they often contribute more than 80% of local catches (see Appendix D). This could represent a large biomass transfer from the High Seas to the coast, if the fish are energetically supported by High Seas primary production through a significant part of their

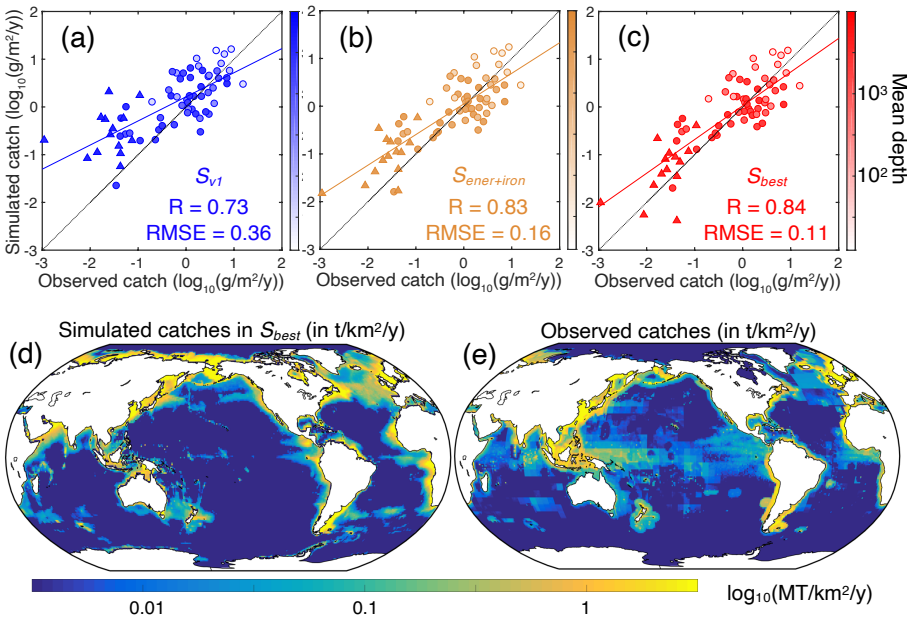

Figure 4. Regional catch variation at the global peak in the 1990s. Observed vs. simulated mean catch densities by regions of the global ocean for: (a) the reference simulations S_{v1}; (b) simulations including ecological features that limit production in the High Seas (HS) $S_{ener+iron}$; (c) simulations including ecological features and economic constraints S_{best}. (d) Map of simulated global catches at peak for the best simulations including ecological and economic features influencing catch in the HS, at global peak. (e) Map of observed global catches at peak. Panel (a-c), the circular markers indicates LMEs, the triangles HSEs (see Appendix F), the lines show linear fits across data, and the shadings indicate variations in the mean depth of each region, on a log10 scale (in m).

life cycle. Assuming that, for example, 50% of straddling catch is derived from High Sea production (i.e., 40% of total catch, where 80% of the catch is straddling) would bring the modelled High Seas to coastal seas catch ratio closer to observations (see S_{mig} Fig. 2a, yellow line). However, to maintain realistic High Seas catches (i.e., about 4 Mt/y), the adjustment of the reference simulation (S_{v1}) would require a migration of more than 60%, which would imply a catch fraction much smaller than observed (1< %, Fig. 2a). Thus, migration could be a very important contributor, but is insufficient alone to explain the small catches in the High Seas.

This analysis highlights the potential for migration of straddling species to naturally extract biomass from the High Seas, since, as long as High Seas biomass density remains lower than coastal seas, migrating biomass will be caught more profitably in coastal regions. When High Seas catches are reduced by lower High Seas biomass (best simulation, S_{best}), correction or remaining discrepancies between the model and observations would require setting 5% of demersal and 10% of pelagic coastal catches on straddling species to come from the High Seas (compare red and yellow lines in Fig. 3). These values modulate the excessive development of High Seas fishing, while allowing realistic High Seas catches (4 Mt/y) and are, therefore, plausible. But migration is hard to constrain, and more work is required to link regions of biomass production to biomass extraction that goes beyond the scope of this study.

3.5 Small High Seas fish biomass and implications

The small High Seas catch fraction requires that, for the same level of primary production, High Seas produce less biomass of commercially targeted fish (see S_{best} Fig. 2). Based on our results, the dominant mechanism behind this small production is the separation of prey resources for pelagic and demersal communities (ENERGYPATH).

Both prey resources, NPP and PFB, are available at distinct relative abundances in High Seas and coastal seas (see PFB/NPP ratios in Fig. 5a). In coastal seas, demersal resources from particle fluxes are on average 10× less abundant than NPP. This proportion decreases to 100× less abundant in the High Seas, because of the increased dissipation of energy of primary production over deeper water columns. Within each region, other mechanisms must compensate for less abundant demersal resources to allow comparable pelagic and demersal biomass densities (Fig. 5b), ultimately explaining the similar magnitude of demersal and pelagic catches in observations (Fig. 3).

A likely candidate mechanism is that, in demersal communities, the processing of detritus by large detritivores in benthic ecosystems shortens the length of food chains before energy reaches the exploitable demersal fish biomass. In BOATS, food chains are, on average, shorter by 1 to 1.4 trophic levels in coastal and High Seas respectively (Fig. 5c). For an average trophic efficiency of 0.1, such compensation can correct the factor-of-10 discrepancy in coastal seas, but is insufficient to correct the factor-of-100 discrepancy in High Seas. In summary, shorter demersal food chains support larger demersal biomass than pelagic biomass in coastal areas. In the High Seas, a larger proportion of the en-

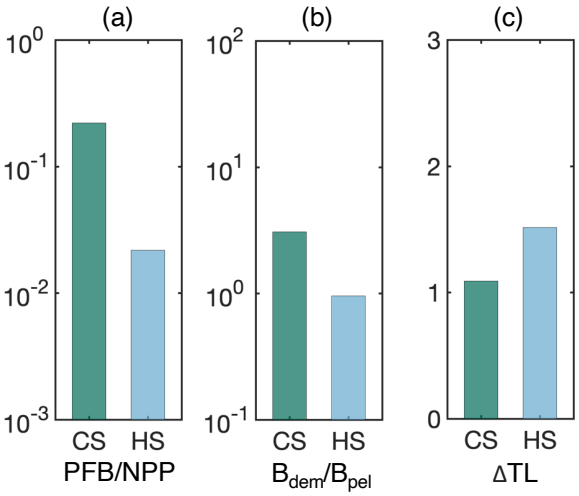

Figure 5. Drivers of the difference in pelagic and demersal biomass. (a) Ratio of low trophic level resources (PFB/NPP) for demersal vs. pelagic communities. (b) Demersal vs. pelagic biomass ratio (B_{dem}/B_{pel}). (c) Trophic distance of fish recruits relative to the representative size of the low trophic level prey. Each unit indicates one additional trophic level for the pelagic community relative to the demersal community. Green and blue bars show coastal (CS) and High Seas (HS) respectively. The ratios are means for the global ocean, weighted by fish biomass and with masked HNLC regions.

ergy available from photosynthesis is lost, leading to a smaller biomass density per unit of NPP.

Our best simulation shows a notable contrast in the change of biomass over time between High Seas and coastal waters. In the early 20th century, the total biomass of commercially-targeted fish in coastal waters is 1.8 Gt, 2-3 times larger than that of the High Seas. The subsequent extraction of commercial fish in coastal regions causes coastal biomass to decline to only 0.8 Gt by 2013 (Fig. 6), a rate of decline comparable to a previous analysis (Worm & Branch, 2012; Bianchi et al., 2021). As a result, the model suggests that the High Seas presently harbor a similar amount of biomass as coastal regions, but spread over a much larger area, and that the fraction of global fish biomass in the High Seas has increased from 30% to 50%. We note that our simulations do not include migrations, which would have caused the High Seas biomass to decrease by a larger amount. Without effective fisheries management (i.e., under open-access dynamics), economic theory suggests that fishing will eventually even out the biomass distribution across High Seas and coastal regions, and continual increases in price and/or technological progress will render previously unprofitable regions suitable for exploitation (compare High Seas and coastal seas biomass in Fig. 6).

4 Conclusion

We shed light on why so few fish are caught in the High Seas by testing a suite of hypotheses using a global fisheries model constrained by global catch observations. Our

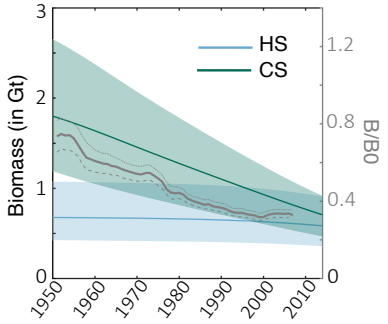

Figure 6. Historical evolution of global biomass under fishing. The green and blue colors show coastal and High Seas respectively, the envelopes the 10-90th percentile ranges for each simulation set, and the gray lines the observed change in biomass based on stock assessments (Worm & Branch, 2012).

results indicate that the primary factor is simply that the biomass of commercially targeted fish in the High Seas is small compared to that of coastal waters. This is an important insight for global marine ecosystem modeling efforts (Lotze et al., 2019; Tittensor et al., 2021) as many models predict large High Seas biomass fraction (see the mean of FishMIP ensemble in Fig. 1a). Our simulations provide ecologically feasible mechanisms to explain this discrepancy, including the dependence of trophic pathways on water depth, and micronutrient limitation. Economic constraints alone cannot explain the low fish catches in the High Seas, but likely modulate the rate of development of High Seas fisheries. Finally, migration of straddling species from the High Seas to coastal regions is difficult to represent and quantify, but is likely to play a significant role in depleting High Seas fish populations by exposing them to fishing effort in coastal waters. In essence, a significant fraction of High Seas fish may be caught when they migrate to coastal waters, without the need to fish far from port.

We suggest that the most important ecological factor explaining the low High Seas catches is the impact of water depth on organic matter consumption (Buesseler & Boyd, 2009). In coastal seas, the concentration of organic production in a thin layer, with fewer trophic steps between primary producers and commercial fish, allows a much larger portion of the energy to be channeled to the large organisms humans prefer to eat, and supports demersal species that dominate on upper shelf slopes (Haedrich & Merrett, 1992; Stasko et al., 2016). In the High Seas, the outputs of primary production are volumetrically diluted, and are consequently consumed by microbes and filter feeders over an extended vertical range of the water column, without accumulating in sufficiently high density to support abundant populations of large fish. Note that mechanisms that couple pelagic and demersal communities could modulate this difference, such as vertical migrations that enable predator-prey interactions across overlapping vertical habitats (Sutton et al., 2008; Trueman et al., 2014). The lack of trace nutrients may also contribute to the sparsity of the pelagic community, for example the low availability of the essential element iron in waters far from shore (Galbraith et al., 2019). As a result, there are fewer

commercially valuable fish to be found in the High Seas. We note that small mesopelagic fish may be abundant in the High Seas, particularly where primary production is elevated (Irigoien et al., 2014; Proud et al., 2018). The relatively high abundances of mesopelagic fish can be attributed to their ability to intercept dispersed sinking fluxes, and a lower susceptibility to iron limitation (Le Mézo & Galbraith, 2021). We have not attempted to explicitly quantify mesopelagic fish here given that they are not commercially exploited at present and therefore cannot be constrained by catch records, a key part of our methodology.

Our results support prior work emphasizing that the High Seas cannot provide a significant amount of wild fish for direct human consumption (Sumaila et al., 2015; Schiller et al., 2018). Although wild fish are relatively nutrient-rich (Golden et al., 2021; Heilpern et al., 2021), the rate at which they are produced is small compared to the overall human food system, which is dominated by terrestrial agriculture (K. J. Scherrer et al., 2023), and the potential of the High Seas to provide additional food is minimal. This is also consistent with historical evidence showing that fisheries in the High Seas have decimated populations of top predators (Cullis-Suzuki & Pauly, 2010; Pacoureau et al., 2021; Juan-Jordá et al., 2022), altering the size structure of the overall community (Hatton et al., 2021), despite providing limited food to humans. Instead of food provision, closing the High Seas to fishing would have the potential benefits of increasing High Seas biodiversity (Gjerde et al., 2016; Sala et al., 2021), reducing fishing gear waste (Helm, 2022), and eliminating costly subsidies and fuel-inefficient fishing practices (White & Costello, 2014; Sala et al., 2018). Timely protection of High Seas ecosystems may help buttress them against increasing pressures to intensify fishing as technological innovations cause them to become financially more attractive despite their low fish biomass density.

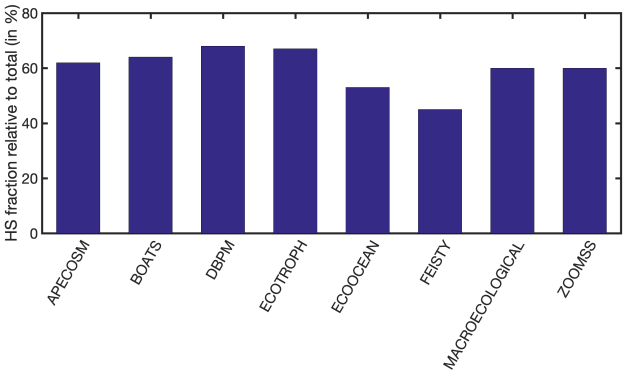

Figure A1. Mean contribution of the High Seas biomass to the global total per FishMIP model of the ISIMIP3b simulations forced with IPSL-CM6A-LR (Tittensor et al., 2021).

Appendix A High seas biomass fraction in FishMIP models

Despite large differences in model structure, global fish biomass models suggest a comparable fraction of High Seas to coastal seas biomass.

Appendix B Variable fishing costs

The cost of fishing varies per fishing gear, per fish community targeted (Lam et al., 2011). To best constrain spatially variable costs we use estimates of these separate fishing costs in the high-seas (HS) for the main gear types (98% of total effort) following data reported by Sala et al. (2018). Table B1 summarizes these estimated costs. These compare with BOATS's default fishing cost of $5.85\$/W/yr$ (Carozza et al., 2017; Galbraith et al., 2017).

Figure B1 summarizes the effect of spatially heterogeneous fishing costs on the ratio HS vs. CS catch, on the variations of the mean depths above which catch occur, as well as the global mean HS fishing cost, once weighted by effort.

First, increasing the cost of fishing with distance to nearest shore [$x^* = 370$,δ_d] can partly correct the ratio of catches between HS and CS (Fig. B1a). But most catch remain over deep seafloor, unlike suggested by observation (mean depth of catch ¡1000m Fig. B1b).

Second, increasing the cost of fishing with seafloor depth [$x^* = 200$,δ_z] can correct both the ratio of catches between HS and CS, and contributes to the shallowing of the mean seafloor depth of catches Figs. B1a,b). But, this correction corresponds to unrealistic high HS fishing costs (¿$8.87\$/W/yr$, upper range of observed costs Fig. B1c), inconsistent with observation (Tab. B1).

In both cases, spatially variable fishing costs within the range of observation can not account for the small fraction of HS vs. CS catches. We tested the effect of separate costs $\delta_{d,z_{bot}}$, adjustment of the parameter x^* only slightly modify the results. For a re-

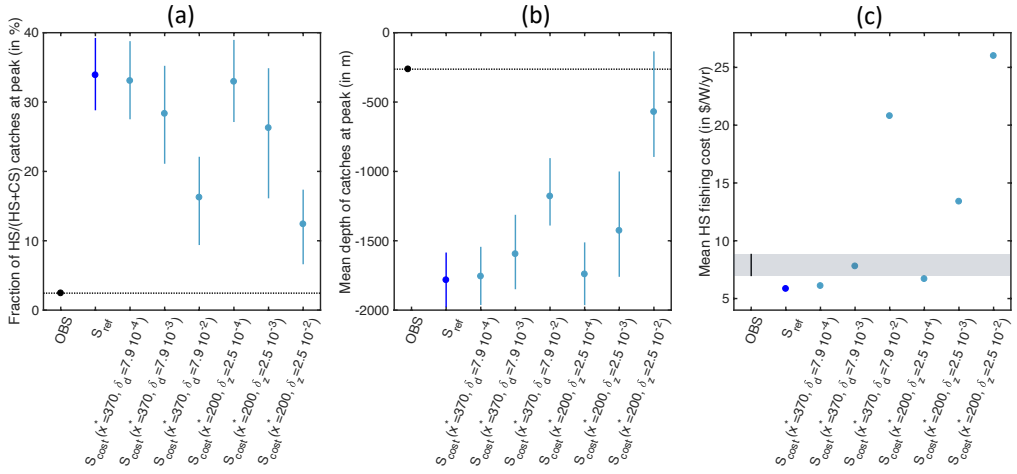

Figure B1. Effect of spatially heterogeneous costs. (a) Observed and simulated fraction of HS vs. CS catches at global peak for multiple model variants. (b) Observed and simulated mean depth of catches at global peak for multiple model variants. (c) Observed and simulated mean HS fishing costs once weighted by local fishing effort, around 2010. Panels (a,b) show the ensemble mean as well as the 25-75th percentile ranges per simulation set compared to observation, black dot and horizontal dotted line. Panel (c) shows mean simulated costs and how they compare to the range of observation Tab. B1 (grey shading).

alistic cost of fishing the high seas the correction of HS vs. CS ratio seems impossible. We conclude that cost alone does not explain the smaller exploitation of the high-seas.

Table B1. Cost of fishing the high-seas based on estimates from Sala et al. (2018) for year 2016.

Gear type	Effort in kWh (fraction of total)	Cost range in $	Cost per unit effort in $\$/W/yr$
Trawlers	979 10^6 (15%)	[750 10^6-1030 10^6]	[6.7-9.2]
Long liners	3719 10^6 (55%)	[2523 10^6-3023 10^6]	[6.0-7.1]
Purse seiners	394 $10^6 s$ (6%)	[702 10^6-1188 10^6]	[15.7-26.0]
Squid jiggers	1490 10^6 (22%)	[1308 10^6-1616 10^6]	[7.7-9.5]
Range all gears	(98%)	-	[6.94-8.87]
BOATS default	-	-	5.85

Appendix C Variable biomass catchabilities

The catchability of fish biomass per unit effort can vary between species (e.g. schooling or dispersed species), depending on the preferred depth inhabited by these species, from the surface to the limit of the euphotic layer depth and to the seafloor. To constrain the spatially variable catchabilities, we compare with estimates of the variability of technology coefficients per fishing gears as detailed in Palomares and Pauly (2019). Table C1

summarizes these estimated coefficients and how they vary. In BOATS the coefficients are spatially homogeneous (value of 1) by default.

Figure C1 summarizes the effect of spatially variable catchabilities on the ratio HS vs. CS catch, and on variations of the mean depths above which catch occur.

The spatial variation of catchability as a function of the depth of the euphotic layer (z_{eu}, $1/z_{eu}$, $log_{10}(z_{eu})$) or seafloor depth (z_{bot}, $log_{10}(z_{bot})$) only allows a limited redistribution of catches from the high seas to the coast (Fig. C1a). The mean depth over which fishing occurs is also partially corrected with each profile (Fig. C1b).

Allowing spatially variable catchabilities while keeping the range within observational ranges (Table C1) does not allow correction of the delayed development of high seas fisheries compared to coastal ones. We conclude that catchability alone can not explain the smaller exploitation of the high-seas. However, slight variations of the catchability could contribute to explain the overall shallow depth of catch, especially when catchability varies with $log_{10}(z_{bot})$ (Fig. C1b).

Table C1. Technology coefficients per fishing gear based on estimates from Palomares and Pauly (2019) for year 1995 (relative to mean).

Gear type	Technology coefficient
Super trawler	1.19
Freeze trawler	0.95
Stern trawler	0.90
Trawlers	0.86
Shrimp trawler	1.05
Tuna seiner	0.76
Tuna longliner	1.10
Purse seiner	0.95
Longliner	1.33
Gillnetter	0.71
Multipurpose	1.19
Range all gears	[0.71-1.33]
BOATS default	1

Appendix D Straddling fraction per EEZ

The migration of fish biomass can influence the spatial correlation of regions where biomass is produced and where it is caught by fisheries. While the straddling fraction of catch in an EEZ does not necessarily reflect the fraction of biomass produced outside this region, it provides an estimate of the plausible range of redistribution. We inferred the straddling catch fraction from Sea Around Us (SAU) reported catch per species within each EEZ, separately summing catch on species solely caught inside EEZs (C^{loc}_{EEZ}), and catch on species caught both in EEZs and highseas (C^{str}_{EEZ}, $\alpha_{str} = C^{str}_{EEZ}/(C^{str}_{EEZ} + C^{loc}_{EEZ})$). We use the list of species in Sumaila et al. (2015) for this distinction. Figure D1a

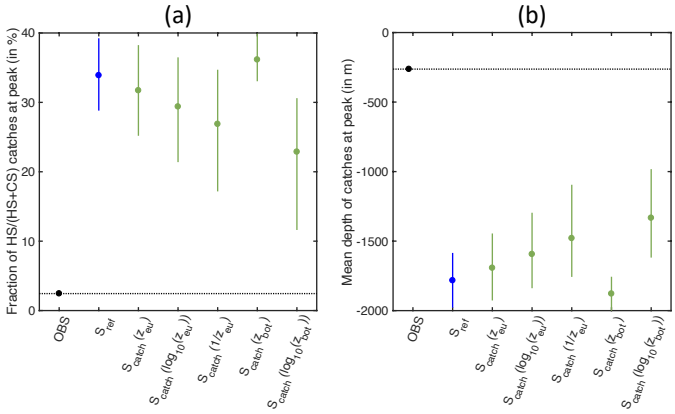

Figure C1. Effect of spatially heterogeneous catchabilities. (a) Observed and simulated fraction of HS vs. CS catches at global peak for multiple model variants. (b) Observed and simulated mean depth of catches at global peak for multiple model variants. Panels (a,b) show the ensemble mean as well as the 25-75th percentile ranges per simulation set compared to observation, black dot and horizontal dotted line.

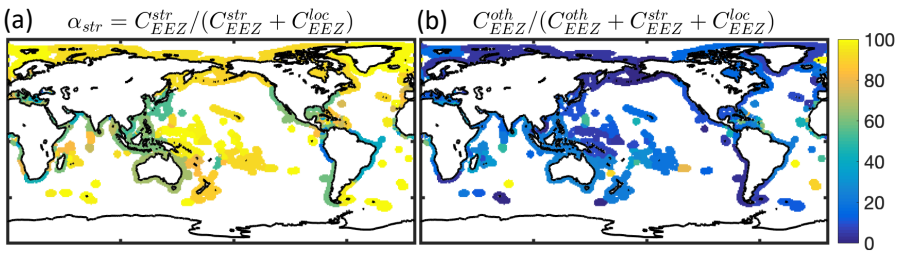

Figure D1. Straddling fraction of catches across EEZs during the 1990s (in %). (a) Fraction of catch on straddling species compared to catch on non straddling species α_{str}. (b) Fraction of catch on species for which the identity is not provided (in %).

shows the estimated mean fraction of straddling catch per LME around the global peak harvest of the 1990s. Note that for each region, a fraction of catch could not be linked to species C^{oth}_{EEZ}, but this fraction is minimal in most EEZs (see Fig. D1b), and thus disregarded in our analysis of the straddling catch fraction.

Figure D2 summarizes the effect of redistributing an increasing ratio δ_s of catch from the HS to the CS, in proportion to the fraction of simulated catch on straddling species α_{str} in each EEZ. It also shows the corresponding annual HS catches.

Increasing δ_s has the expected effect of strongly reducing the HS vs. CS catch fraction (Fig. D2a), up to matching observation for $\delta_s = 0.5$. Despite the improvement, remaining catches in the HS are significantly larger than what is observed (¿4 $10^6 MT/y$, observation around peak of the 1990s, see Fig. D2b). We conclude that the biomass redistribution by migrating species alone does not explain the smaller exploitation of the high seas, nevertheless it must have a significant impact.

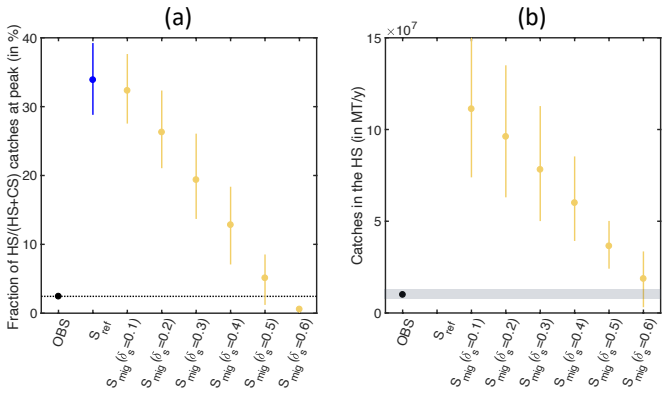

Figure D2. Effect of catch redistribution. (a) Observed and simulated fraction of HS vs. CS catches at global peak for multiple model variants. (b) Annual HS catch around the catch peak of the 1990*s*. Panels (a,b) show the ensemble mean as well as the 25-75th percentile ranges per simulation set compared to observation, black dot and horizontal dotted line.

Appendix E Pelagic and Demersal catches in SAU

We compare simulated pelagic and demersal catches with global catch reconstruction from Sea Around Us (SAU) (Pauly et al., 2020). Table E1 lists how we distribute the functional types of SAU to generate aggregated maps of pelagic and demersal catches.

Table E1. Association of SAU functional types to pelagic and demersal catches.

Catch type	SAU functional types
Pelagic	pelagic s/m/l
	bathypelagic s/m/l
	cephalopods
Demersal	demersal s/m/l
	reef-associated s/m/l
	benthopelagic s/m/l
	bathydemersal s/l
	shark s/l
	flatfish s/l
	ray s/l
	shrimp
	lobster and crab
	other demersal invertebrates

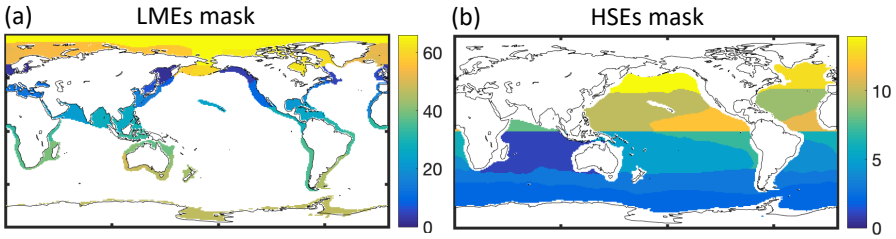

Figure F1. Regional masks to compare observation and simulation. (a) Large Marine Ecosystems. (b) High Seas Ecosystems adapted from Weber et al. (2016).

Appendix F Large Marine Ecosystems and High Seas Ecosystems

Catch are compared across Large Marine Ecosystems (LMEs) for coastal regions, and 11 High Seas Ecosystems (HSEs). Figure F1a, b illustrate respectively the LME and HSE masks.

Open Research Section

All data and the model used in this study are publicly available. Catch observation used for comparison of simulations can be obtained from the links `https://www.seaaroundus.org` and `http://dx.doi.org/10.4226/77/58293083b0515`. Biomass simulations from FishMIP can be obtained from the link `https://www.isimip.org/outputdata/`. Other processed data, as well as the code of the model BOATS used for this analysis, are available at the link `https://zenodo.org/records/10662929`.

Acknowledgments

D.B. and J.G. acknowledge support from the US National Aeronautics and Space Administration (NASA) grant 80NSSC21K0420. Computational resources were provided by the Expanse system at the San Diego Supercomputer Center through allocation TG-OCE170017 from the Advanced Cyber infrastructure Coordination Ecosystem: Services and Support (ACCESS) program, which is supported by National Science Foundation grants 2138259, 2138286, 2138307, 2137603, and 2138296. E.D.G. was supported by the Canada Research Chairs Program fund number CRC-2020-00108. K.J.N.S was supported by the Norwegian Research Council, project 326896.

References

Amante, C., & Eakins, B. W. (2009). Etopo1 arc-minute global relief model: procedures, data sources and analysis.

Bar-On, Y. M., Phillips, R., & Milo, R. (2018). The biomass distribution on earth. *Proceedings of the National Academy of Sciences*, *115*(25), 6506–6511.

Behrenfeld, M. J., & Falkowski, P. G. (1997). Photosynthetic rates derived from satellite-based chlorophyll concentration. *Limnology and Oceanography*, *42*(1),

1–20.

Bianchi, D., Carozza, D. A., Galbraith, E. D., Guiet, J., & DeVries, T. (2021). Estimating global biomass and biogeochemical cycling of marine fish with and without fishing. *Science advances*, *7*(41), eabd7554.

Blanchard, J. L., Heneghan, R. F., Everett, J. D., Trebilco, R., & Richardson, A. J. (2017). From bacteria to whales: Using functional size spectra to model marine ecosystems. *Trends in Ecology & Evolution*, *32*(3), 174-186. doi: 10.1016/j.tree.2016.12.003

Blanchard, J. L., Law, R., Castle, M. D., & Jennings, S. (2011). Coupled energy pathways and the resilience of size-structured food webs. *Theoretical Ecology*, *4*(3), 289-300. doi: 10.1007/s12080-010-0078-9

Block, B. A., Jonsen, I. D., Jorgensen, S. J., Winship, A. J., Shaffer, S. A., Bograd, S. J., ... others (2011). Tracking apex marine predator movements in a dynamic ocean. *Nature*, *475*(7354), 86.

Buesseler, K. O., & Boyd, P. W. (2009). Shedding light on processes that control particle export and flux attenuation in the twilight zone of the open ocean. *Limnology and Oceanography*, *54*(4), 1210–1232.

Carozza, D. A., Bianchi, D., & Galbraith, E. D. (2016). The ecological module of BOATS-1.0: a bioenergetically constrained model of marine upper trophic levels suitable for studies of fisheries and ocean biogeochemistry. *Geoscientific Model Development*, *9*(4), 1545–1565.

Carozza, D. A., Bianchi, D., & Galbraith, E. D. (2017, 01). Formulation, general features and global calibration of a bioenergetically-constrained fishery model. *PLOS One*, *12*(1), 1-28. doi: 10.1371/journal.pone.0169763

Carr, M.-E., Friedrichs, M. A., Schmeltz, M., Aita, M. N., Antoine, D., Arrigo, K. R., ... others (2006). A comparison of global estimates of marine primary production from ocean color. *Deep Sea Research Part II: Topical Studies in Oceanography*, *53*(5), 741–770.

Cullis-Suzuki, S., & Pauly, D. (2010). Failing the high seas: A global evaluation of regional fisheries management organizations. *Marine Policy*, *34*(5), 1036 - 1042. doi: https://doi.org/10.1016/j.marpol.2010.03.002

Dunne, J. P., Armstrong, R. A., Gnanadesikan, A., & Sarmiento, J. L. (2005). Empirical and mechanistic models for the particle export ratio. *Global Biogeochemical Cycles*, *19*(4).

Eddy, T. D., Bernhardt, J. R., Blanchard, J. L., Cheung, W. W., Colléter, M., Du Pontavice, H., ... others (2020). Energy flow through marine ecosystems: Confronting transfer efficiency. *Trends in Ecology & Evolution*.

Eigaard, O. R., Marchal, P., Gislason, H., & Rijnsdorp, A. D. (2014). Technological development and fisheries management. *Reviews in Fisheries Science & Aquaculture*, *22*(2), 156–174.

Galbraith, E. D., Carozza, D. A., & Bianchi, D. (2017). A coupled human-earth model perspective on long-term trends in the global marine fishery. *Nature Communications*, *8*, 14884.

Galbraith, E. D., Le Mézo, P., Solanes Hernandez, G., Bianchi, D., & Kroodsma, D.

(2019). Growth limitation of marine fish by low iron availability in the open ocean. *Frontiers in Marine Science*, 509.

Gjerde, K., Reeve, L., Harden-Davies, H., Ardron, J., Dolan, R., Durussel, C., ... others (2016). Protecting earth's last conservation frontier: scientific, management and legal priorities for mpas beyond national boundaries.

Golden, C. D., Koehn, J. Z., Shepon, A., Passarelli, S., Free, C. M., Viana, D. F., ... others (2021). Aquatic foods to nourish nations. *Nature*, *598*(7880), 315–320.

Guiet, J., Aumont, O., Poggiale, J.-C., & Maury, O. (2016). Effects of lower trophic level biomass and water temperature on fish communities: A modelling study. *Progress in Oceanography*, *146*, 22 - 37. doi: http://dx.doi.org/10.1016/j.pocean.2016.04.003

Guiet, J., Bianchi, D., Scherrer, K. J., Heneghan, R. F., & Galbraith, E. D. (2024). Boatsv2: New ecological and economic features improve simulations of high seas catch and effort. *Submitted in Geoscientific Model Development*.

Guiet, J., Galbraith, E. D., Bianchi, D., & Cheung, W. W. (2020). Bioenergetic influence on the historical development and decline of industrial fisheries. *ICES Journal of Marine Science*, *77*(5), 1854–1863.

Haedrich, R. L., & Merrett, N. R. (1992). Production/biomass ratios, size frequencies and biomass spectra in deep-sea demersal fishes. In *Deep-sea food chains and the global carbon cycle* (pp. 157–182). Springer.

Hatton, I. A., Heneghan, R. F., Bar-On, Y. M., & Galbraith, E. D. (2021). The global ocean size spectrum from bacteria to whales. *Science Advances*, *7*(46), eabh3732. doi: 10.1126/sciadv.abh3732

Heilpern, S. A., DeFries, R., Fiorella, K., Flecker, A., Sethi, S. A., Uriarte, M., & Naeem, S. (2021). Declining diversity of wild-caught species puts dietary nutrient supplies at risk. *Science Advances*, *7*(22), eabf9967.

Helm, R. R. (2022). Turning the tide on high-seas plastic pollution. *One Earth*, *5*(10), 1089–1092.

Heneghan, R. F., Galbraith, E., Blanchard, J. L., Harrison, C., Barrier, N., Bulman, C., ... others (2021). Disentangling diverse responses to climate change among global marine ecosystem models. *Progress in Oceanography*, *198*, 102659.

Irigoien, X., Klevjer, T. A., Røstad, A., Martinez, U., Boyra, G., & et al., A. J. L. (2014). Large mesopelagic fishes biomass and trophic efficiency in the open ocean. *Nature Communications*, *5*.

Juan-Jordá, M. J., Murua, H., Arrizabalaga, H., Merino, G., Pacoureau, N., & Dulvy, N. K. (2022). Seventy years of tunas, billfishes, and sharks as sentinels of global ocean health. *Science*, *378*(6620), eabj0211.

Kerry, C. R., Exeter, O. M., & Witt, M. J. (2022). Monitoring global fishing activity in proximity to seamounts using automatic identification systems. *Fish and Fisheries*, *23*(3), 733–749.

Kvile, K. Ø., Taranto, G. H., Pitcher, T. J., & Morato, T. (2014). A global assessment of seamount ecosystems knowledge using an ecosystem evaluation framework. *Biological Conservation*, *173*, 108–120.

Lam, V. W. Y., Sumaila, U. R., Dyck, A., Pauly, D., & Watson, R. (2011). Con-

struction and first applications of a global cost of fishing database. *ICES Journal of Marine Science*, *68*(9), 1996-2004. doi: 10.1093/icesjms/fsr121

Le Mézo, P. K., & Galbraith, E. D. (2021). The fecal iron pump: global impact of animals on the iron stoichiometry of marine sinking particles. *Limnology and Oceanography*, *66*(1), 201–213.

Locarnini, R. A., Mishonov, A. V., Antonov, J. I., Boyer, T. P., & Garcia, H. E. (2006). World ocean atlas 2005, volume 1: Temperature. s. levitus. *Ed. NOAA Atlas NESDIS 61, U.S. Government Printing Office, Washington, D.C., 182 pp*.

Lotze, H. K., Tittensor, D. P., Bryndum-Buchholz, A., Eddy, T. D., Cheung, W. W. L., Galbraith, E. D., ... Worm, B. (2019). Global ensemble projections reveal trophic amplification of ocean biomass declines with climate change. *Proceedings of the National Academy of Sciences*. doi: 10.1073/pnas.1900194116

Marra, J., Trees, C. C., & O'Reilly, J. E. (2007). Phytoplankton pigment absorption: a strong predictor of primary productivity in the surface ocean. *Deep Sea Research Part I: Oceanographic Research Papers*, *54*(2), 155–163.

Martin, J. H., Knauer, G. A., Karl, D. M., & Broenkow, W. W. (1987). Vertex: carbon cycling in the northeast pacific. *Deep Sea Research Part A. Oceanographic Research Papers*, *34*(2), 267–285.

Maury, O. (2010). An overview of apecosm, a spatialized mass balanced "apex predators ecosystem model" to study physiologically structured tuna population dynamics in their ecosystem. *Progress in Oceanography*, *84*(1-2), 113–117.

Moore, C., Mills, M., Arrigo, K., Berman-Frank, I., Bopp, L., Boyd, P., ... others (2013). Processes and patterns of oceanic nutrient limitation. *Nature geoscience*, *6*(9), 701–710.

Nuno, A., Guiet, J., Baranek, B., & Bianchi, D. (2022). Patterns and drivers of the diving behavior of large pelagic predators. *bioRxiv*. doi: https://doi.org/10.1101/2022.12.27.521953

Pacoureau, N., Rigby, C. L., Kyne, P. M., Sherley, R. B., Winker, H., Carlson, J. K., ... others (2021). Half a century of global decline in oceanic sharks and rays. *Nature*, *589*(7843), 567–571.

Palomares, M. L., & Pauly, D. (2019). On the creeping increase of vessels' fishing power. *Ecology and Society*, *24*(3).

Pauly, D., Zeller, D., & Palomares, M. (2020). Sea around us concepts, design and data. Retrieved from `seaaroundus.org`

Petrik, C. M., Stock, C. A., Andersen, K. H., van Denderen, P. D., & Watson, J. R. (2019). Bottom-up drivers of global patterns of demersal, forage, and pelagic fishes. *Progress in oceanography*, *176*, 102124.

Proud, R., Cox, M. J., Le Guen, C., & Brierley, A. S. (2018). Fine-scale depth structure of pelagic communities throughout the global ocean based on acoustic sound scattering layers. *Marine Ecology Progress Series*, *598*, 35–48.

RAM Legacy Stock Assessment Database. (2020). *Ram legacy stock assessment*

database v4.491. Retrieved from `https://doi.org/10.5281/zenodo.3676088` doi: 10.5281/zenodo.3676088

Rousseau, Y., Watson, R. A., Blanchard, J. L., & Fulton, E. A. (2019). Evolution of global marine fishing fleets and the response of fished resources. *Proceedings of the National Academy of Sciences*, *116*(25), 12238-12243. doi: 10.1073/pnas.1820344116

Sala, E., Mayorga, J., Bradley, D., Cabral, R. B., Atwood, T. B., Auber, A., ... others (2021). Protecting the global ocean for biodiversity, food and climate. *Nature*, *592*(7854), 397–402.

Sala, E., Mayorga, J., Costello, C., Kroodsma, D., Palomares, M. L., Pauly, D., ... Zeller, D. (2018). The economics of fishing the high seas. *Science advances*, *4*(6), eaat2504.

Scherrer, K., & Galbraith, E. D. (2020). Regulation strength and technology creep play key roles in global long-term projections of wild capture fisheries. *ICES Journal of Marine Science*. doi: 10.1093/icesjms/fsaa109

Scherrer, K. J., Rousseau, Y., Teh, L. C., Sumaila, U. R., & Galbraith, E. D. (2023). Diminishing returns on labour in the global marine food system. *Nature Sustainability*, 1–8.

Schiller, L., Bailey, M., Jacquet, J., & Sala, E. (2018). High seas fisheries play a negligible role in addressing global food security. *Science Advances*, *4*(8), eaat8351.

Stasko, A. D., Swanson, H., Majewski, A., Atchison, S., Reist, J., & Power, M. (2016). Influences of depth and pelagic subsidies on the size-based trophic structure of beaufort sea fish communities. *Marine Ecology Progress Series*, *549*, 153–166.

Stock, C. A., John, J. G., Rykaczewski, R. R., Asch, R. G., Cheung, W. W. L., Dunne, J. P., ... Watson, R. A. (2017). Reconciling fisheries catch and ocean productivity. *Proceedings of the National Academy of Sciences*, *114*(8), E1441-E1449. doi: 10.1073/pnas.1610238114

Sumaila, U. R., Lam, V. W., Miller, D. D., Teh, L., Watson, R. A., Zeller, D., ... others (2015). Winners and losers in a world where the high seas is closed to fishing. *Scientific Reports*, *5*(1), 1–6.

Sutton, T., Porteiro, F., Heino, M., Byrkjedal, I., Langhelle, G., Anderson, C., ... others (2008). Vertical structure, biomass and topographic association of deep-pelagic fishes in relation to a mid-ocean ridge system. *Deep Sea Research Part II: Topical Studies in Oceanography*, *55*(1-2), 161–184.

Tagliabue, A., Bowie, A. R., Boyd, P. W., Buck, K. N., Johnson, K. S., & Saito, M. A. (2017). The integral role of iron in ocean biogeochemistry. *Nature*, *543*(7643), 51–59.

Tittensor, D. P., Eddy, T. D., Lotze, H. K., Galbraith, E. D., Cheung, W., Barange, M., ... others (2018). A protocol for the intercomparison of marine fishery and ecosystem models: Fish-mip v1. 0. *Geoscientific Model Development*, *11*(4), 1421–1442.

Tittensor, D. P., Novaglio, C., Harrison, C. S., Heneghan, R. F., Barrier, N.,

Bianchi, D., ... others (2021). Next-generation ensemble projections reveal higher climate risks for marine ecosystems. *Nature Climate Change*, *11*(11), 973–981.

Trueman, C., Johnston, G., O'hea, B., & MacKenzie, K. (2014). Trophic interactions of fish communities at midwater depths enhance long-term carbon storage and benthic production on continental slopes. *Proceedings of the Royal Society B: Biological Sciences*, *281*(1787), 20140669.

van Denderen, P. D., Lindegren, M., MacKenzie, B. R., Watson, R. A., & Andersen, K. H. (2018). Global patterns in marine predatory fish. *Nature ecology & evolution*, *2*(1), 65.

Watson, R. A. (2017). A database of global marine commercial, small-scale, illegal and unreported fisheries catch 1950–2014. *Scientific Data*, *4*.

Watson, R. A., & Morato, T. (2013). Fishing down the deep: Accounting for within-species changes in depth of fishing. *Fisheries Research*, *140*, 63–65.

Weber, T., Cram, J. A., Leung, S. W., DeVries, T., & Deutsch, C. (2016). Deep ocean nutrients imply large latitudinal variation in particle transfer efficiency. *Proceedings of the National Academy of Sciences*, *113*(31), 8606–8611.

White, C., & Costello, C. (2014). Close the high seas to fishing? *PLoS biology*, *12*(3), e1001826.

Worm, B., & Branch, T. A. (2012). The future of fish. *Trends in Ecology & Evolution*, *27*(11), 594 - 599. doi: https://doi.org/10.1016/j.tree.2012.07.005